Dept. of Math./CMA Univ. of Oslo
Pure Mathematics No 6
ISSN 0806–2439 March 2009

ELECTROWETTING OF A 3D DROP: NUMERICAL MODELLING WITH ELECTROSTATIC VECTOR FIELDS

Patrick Ciarlet, Jr.[1] and Claire Scheid[2]

Abstract. The electrowetting process is commonly used to handle very small amounts of liquid on a solid surface. This process can be modelled mathematically with the help of the shape optimization theory. However, solving numerically the resulting shape optimization problem is a very complex issue, even for reduced models that occur in simplified geometries. Recently, the second author obtained convincing results in the 2D axisymmetric case. In this paper, we propose and analyze a method that is suitable for the full 3D case.

1991 Mathematics Subject Classification. 65N12, 65N30, 49Q10.

.

Introduction

Handling very small amounts of liquid on a solid surface is of industrial interest, especially in microfluidics. In this field, electrowetting process is now broadly used. Indeed, the typical experiment consists in charging a droplet posed on a solid by applying a given voltage between this droplet and a counter-electrode placed beneath the insulator (see figure 1). This allows one to quickly control the wetting of the drop on the solid at small costs. Thus a wide range of applications already exists: from variable focal liquid lenses (Varioptic; B. Berge, Philips...), to "lab on a chip" and microchip (see e.g. : http://www-leti.cea.fr; Y. Fouillet, http:www.cem.ucla.edu/; R. Garrell's group...). The literature on this topic is developed as well; most of it is devoted to experimental aspects.

When one lets the applied voltage vary, experiments show a locking phenomenon: after a critical value of the voltage has been reached, the shape of the drop remains fixed. Explaining this locking phenomenon is still an open question: this could be due to droplet ejection, insulator breakdown, ionization of the air (see for example Refs. [24, 25, 30, 31]...).

Concerning modelling, a first approximate model is commonly used. Called the *plane capacitor approximation*, it amounts to consider that the system is a plane capacitor. Thus one can describe the behavior of the drop at a given applied voltage. This model has been validated by experiments at small voltages. But it predicts a total spreading of the drop as the voltage increases, in contradiction with the locking phenomenon described above.

Keywords and phrases: electrowetting, energy minimization, contact angle, error estimates

[1] Laboratoire POEMS, UMR 2706 CNRS/ENSTA/INRIA,
ENSTA ParisTech,
32, boulevard Victor, 75739 Paris Cedex 15, France
patrick.ciarlet@ensta.fr

[2] CMA c/o Dept. of Math. University of Oslo
P.O. Box 1053 Blindern
NO-0316 Oslo, Norway
claire.scheid@cma.uio.no

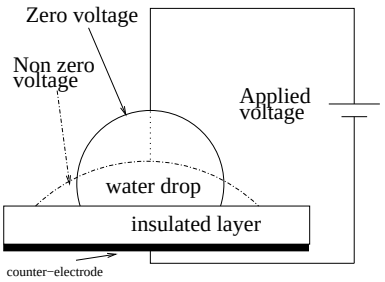

FIGURE 1. Principle of Electrowetting

Due to the shape of the drop, the electric field, created by the application of the voltage, is singular at the interface between liquid, solid and gas (the so-called *triple line*). This fact is usually put forward, when one tries to understand the electrowetting process as well as its locking. In particular one needs to describe more precisely the geometry of the drop near the triple line. In this prospect, Buerhle *et al* in [5] considered a second approximate model for the drop near the triple line: the drop is viewed as a 2D section of cylindrical 3D drop infinite in the direction perpendicular to the section. A physical analysis of this model yields a surprising result: the *contact angle* (the angle between the drop and the solid at the triple line) should remain constant, independently of the applied voltage.

Mathematically speaking, a shape optimization modelling of electrowetting, based on energy minimization and valid in a 3D geometry, can be used (cf. [3]).

This full model has been studied in the 3D axisymmetric case. Indeed, when the shape of the drop is invariant by rotation, the problem can then be recast in a 2D setting as data automatically become invariant by rotation. The invariance of the contact angle with respect to the applied voltage has been proved theoretically in [28]. Numerical aspects have also been investigated in this particular case. In order to be able to observe numerically the invariance of the contact angle, it was required to adopt a microscopic point of view in the model to focus on the *triple line*. And then, as the electrostatic potential is singular there, to treat its singular behavior with special care: it has been calculated in [27] using a singularity treatment: the Singular Complement Method (SCM, see for instance [8]). As a matter of fact, the use of the SCM greatly improves the quality of the numerical computations, compared to approximations based on refined meshes (see [27]).

In the light of the above mentioned results, it is clear that the axisymmetric case is a first important step. But as non-axisymmetric shapes can also be observed in reality, the study of the full model, i.e. in 3D geometries without *a priori* symmetry, is of central importance.

Numerically speaking, a precise calculus of the electrostatic potential is also needed for this full model. The use of a generalized Singular Complement Method is *a priori* an interesting choice (see [3]). However, one has to deal with the approximation of a Singular Complement that belongs to an infinite-dimensional vector space in 3D settings, instead of a one-dimensional vector space in 2D settings. The resulting numerical method is therefore much more costly to implement. Also, numerical experiments on a sample test-case (in [17]) show that the 3D implementation is not as efficient as its 2D counterpart. Or, rather than calculate the electrostatic potential, one can choose instead to compute directly the electrostatic field, to improve the quality of the numerical approximation. This can be achieved *via* a weighted weak formulation (see [7, 12]). Indeed, this approach works in general geometries ([10]). In this paper, we focus on this method.

The rest of the paper is organized as follows. The first part deals with the more theoretical features: it is dedicated to the energy minimization modelling of the electrowetting process (cf. [3]), and it is used on 3D geometries. Notations are set in §1.1, and the model is solved with the help of the shape optimization theory in §1.2. In particular, necessary conditions for optimality are derived. Then in §1.3, we concentrate on the

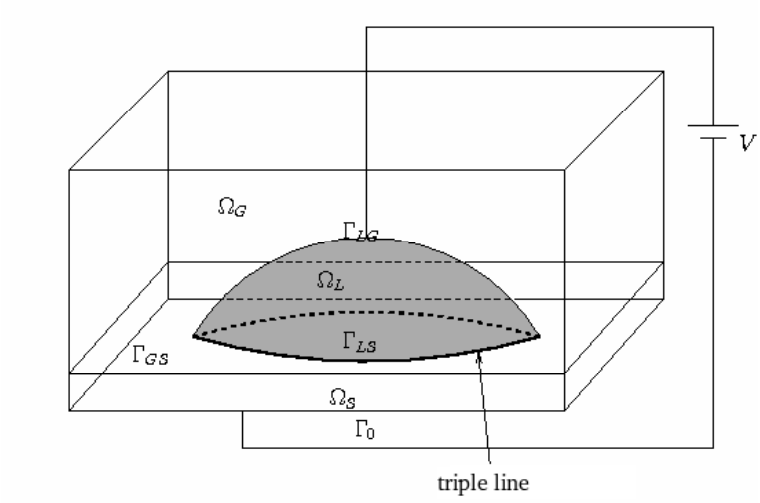

FIGURE 2. The 3D domain

generalization of a result already obtained in the 2D case, namely, that the contact angle is independent of the applied voltage. The second part of the paper focuses on a new characterization of the electrostatic field, and on its numerical analysis. First, we recall how one can reduce the shape optimization problem to a series of computations of the field on varying geometries. This problem is then recast as a weighted weak formulation, see §2.2, and the approximation with conforming nodal finite element is investigated in §2.3. Finally, in §2.4, we review some other discretization techniques.

1. Modelling electrowetting in 3D

We study the evolution of the shape of a droplet, submitted to a voltage, posed on an insulated polymer (the experimental device). The upper face of the polymer film, on which the drop is posed, rests in the plane (Oxy). We call Ω_e the bounded domain of $\mathbb{R}^3$ in which the experiment takes place and in which the calculations are carried out.

1.1. **Notations**

Let $\cdot$ be the scalar product, and let $|\cdot|$ be the norm of vectors of $\mathbb{R}^3$.

Domains and boundaries. We use indices L, S and G to refer to liquid, solid and gas domains respectively. A couple of indices LS, LG... refers to a liquid-solid, liquid-gas interaction respectively. Let:

- Ω_L be the domain of $\mathbb{R}^3$ occupied by the liquid and Γ_L its boundary ;
- Γ_{LS} be the liquid-solid interface ;
- Γ_{LG} be the liquid-gas interface ;
- Ω_G be the domain of $\mathbb{R}^3$ occupied by the gas phase and Γ_G its boundary ;
- Ω_S be the domain of $\mathbb{R}^3$ occupied by the solid and Γ_S its boundary ;
- Γ_0 be the boundary of Ω_e where the counter-electrode is applied ;
- $\Gamma_{ext} = \partial\Omega_e \setminus \overline{\Gamma}_0$ be the exterior boundary of Ω_e.

The domain $\Omega = \Omega_e \setminus \overline{\Omega}_L$ (the exterior of the drop) will be of central importance.
Ω_S, Ω_G, Ω_L, Ω are included in Ω_e.

The liquid-solid-gas interface is called the **triple line** and it is denoted by Γ.

Physical parameters.

- ε_G, ε_S and ε_L are the constant permittivities of Ω_G, Ω_S and Ω_L. The global permittivity ε is defined on Ω by $\varepsilon_{|\Omega_i} = \varepsilon_i$, for $i = G, S, L$.
- σ_{LS}, σ_{GS} and σ_{LG} are the constant surface tensions at the interfaces.
- vol is the given volume of the considered drop.
- g is the gravity.

More generally, if F is a function defined on Ω, we will denote by F_G its restriction on Ω_G, and by F_S its restriction on Ω_S.

1.2. **The optimal shape problem**

The electrowetting modelling is studied in details in [28], with an electrostatic potential point of view. That is: the potential created by the application of a given voltage is calculated. Here we choose a slightly different point of view. As we will see later, we only need to determine accurately the electrostatic field. So we decide rather to focus on the direct calculation of the electrostatic field instead of the electrostatic potential. This gives exactly the same theoretical results as we will see later on.

Electrostatic field. Applying a voltage V between the drop Ω_L and the counter-electrode Γ_0 creates an electrostatic potential χ in the whole space $\mathbb{R}^3$, together with an electrostatic field $\mathbf{E} = \nabla\chi$. As the drop is supposed to be perfectly conductive (formally, $\varepsilon_L = \infty$), χ is constant in Ω_L and so $\mathbf{E}$ is zero in Ω_L. The voltage V is by definition equal to the difference between the applied potential on Ω_L and the applied potential on Γ_0. Since we focus on the electrostatic field, we remark that we can choose the applied potentials up to any given constant value. As a matter of fact, we can consider that the applied potential is $V + v$ on Ω_L, and v on Γ_0, with any value of the constant v, and obtain the same field $\mathbf{E}$. On the other hand, the potential χ is modified by a constant, namely v. So we consider from now on that the applied potential is 0 on Ω_L, and $-V$ on Γ_0.

We neglect electrostatic effects far away from the drop, which has an incidence on the chosen boundary condition on the exterior boundary Γ_{ext} (see (6) below).

We denote by $\mathbf{E}^\Omega$ the electrostatic field created in the exterior of the drop Ω_L i.e. in Ω. It is then governed by

$$\begin{aligned}
\mathbf{curl}\,\mathbf{E}_i^\Omega &= 0 \text{ in } \Omega_i, \text{ where } i = G, S, && (1)\\
\operatorname{div}(\varepsilon_i \mathbf{E}_i^\Omega) &= 0 \text{ in } \Omega_i, \text{ where } i = G, S, && (2)\\
\mathbf{E}^\Omega \times \mathbf{n} &= 0 \text{ on } \Gamma_L \cup \Gamma_0, && (3)\\
\varepsilon_G \mathbf{E}_G^\Omega \cdot \mathbf{n} &= \varepsilon_S \mathbf{E}_S^\Omega \cdot \mathbf{n} \text{ on } \Gamma_{GS}, && (4)\\
\mathbf{E}_G^\Omega \times \mathbf{n} &= \mathbf{E}_S^\Omega \times \mathbf{n} \text{ on } \Gamma_{GS}, && (5)\\
\mathbf{E}^\Omega \cdot \mathbf{n} &= 0 \text{ on } \Gamma_{ext}, && (6)
\end{aligned}$$

where $\mathbf{n}$ is the unit normal vector to Γ_{GS}, exterior to Ω_G.

Eqs (1)-(6) do not characterize completely $\mathbf{E}^\Omega$ (V does not appear!), however we know the structure of solutions to this system. Indeed, the domain Ω under consideration is simply connected but, on the other hand, its boundary is not connected (it has two connected components Γ_0 and Γ_L). Following [14], $\mathbf{E}^\Omega$ can be expressed as

$$E^\Omega = -V\nabla\chi_0^\Omega \qquad (7)$$

where χ_0^Ω is governed by

$$\left\{\begin{array}{l} \mathrm{div}\,(\varepsilon_i \nabla \chi_{0,i}^\Omega) = 0 \text{ in } \Omega_i \quad i = 0, L \\ \chi_{0,i}^\Omega = \delta_{i0} \text{ on } \Gamma_i \quad i = 0, L \\ \varepsilon_G \nabla \chi_{0,G}^\Omega \cdot \mathbf{n} = \varepsilon_S \nabla \chi_{0,S}^\Omega \cdot \mathbf{n} \text{ on } \Gamma_{GS} \\ \chi_{0,G}^\Omega = \chi_{0,S}^\Omega \text{ on } \Gamma_{GS} \\ \nabla \chi_0^\Omega \cdot \mathbf{n} = 0 \text{ on } \Gamma_{ext} \end{array}\right. .$$

If we introduce the one-by-one capacitance matrix of the system, i.e. the scalar

$$\mathbb{C} = \int_\Omega \varepsilon \nabla \chi_0^\Omega \cdot \nabla \chi_0^\Omega \, d\Omega,$$

one can check easily that

$$\int_{\Gamma_0} \varepsilon \mathbf{E}^\Omega \cdot \mathbf{n} \, d\Gamma = -\mathbb{C}V. \tag{8}$$

From [14], we know that (1)-(6) and (8) characterize completely $\mathbf{E}^\Omega$.

Remark 1.1. *The field $\mathbf{E}^\Omega$ is singular at the triple line, due to the geometry there. The relation (7) allows us to derive the regularity of $\mathbf{E}^\Omega$ (in terms of Sobolev spaces), using the theory of regularity of solutions to elliptic PDE's (cf. [22, 23]).*

Minimization of the energy. Several forces act on the drop. Gravitational forces due to the weight of the drop, capillary forces due to surface tension at all the interfaces, electrostatic forces due to the application of a voltage. The system tends to reach its equilibrium which is the minimum of its free energy. For a given applied voltage V, the latter is then given by:

$$\mathcal{E}(\Omega_L, V) := J(\Omega) := \underbrace{\rho g \int_{\Omega_L} z \, d\Omega}_{\text{Potential energy}} + \underbrace{\int_{\Gamma_{LG}} \sigma_{LG} \, d\Gamma + \int_{\Gamma_{LS}} \sigma_{LS} \, d\Gamma + \int_{\Gamma_{GS}} \sigma_{GS} \, d\Gamma}_{\text{Capillary energy}} - \underbrace{\frac{1}{2} \int_\Omega \varepsilon |\mathbf{E}^\Omega|^2 \, d\Omega.}_{\text{Electrostatic energy}}$$

The minus sign in front of the electrostatic energy comes from the fact that the voltage is applied by an external generator. The interested reader can find details and motivation on models on electrowetting in Refs. [2,19].

The problem is then:
For a given volume *vol* and a given voltage V, find Ω_L^* the *shape of a drop* (or equivalently, find Ω^*), such that:

$$\mathcal{E}(\Omega_L^*, V) = \min_{\{\Omega_L \,|\, \mathrm{volume}(\Omega_L) = vol\}} \mathcal{E}(\Omega_L, V) = \min_{\{\Omega \,|\, \mathrm{volume}(\Omega_L) = vol\}} J(\Omega)$$

Remark 1.2. *The meaning of the phrase shape of a drop will be specified in the next paragraph.*

By introducing the scaling parameters,

$$\alpha = \frac{\rho g}{\sigma_{LG}}, \quad \mu = \frac{\sigma_{LS} - \sigma_{GS}}{\sigma_{LG}}, \quad \delta = \frac{1}{\sigma_{LG}}, \tag{9}$$

one finds that, up to an additive constant, minimizing the energy is equivalent to minimizing the functional

$$J(\Omega) = \underbrace{-\alpha \int_\Omega z \, d\Omega}_{J_{grav}(\Omega)} + \underbrace{\mu \int_{\Gamma_{LS}} d\Gamma}_{J_{LS}(\Omega)} + \underbrace{\int_{\Gamma_{LG}} d\Gamma}_{J_{LG}(\Omega)} \underbrace{- \frac{\delta}{2} \int_\Omega \varepsilon |\mathbf{E}^\Omega|^2 \, d\Omega}_{J_{elec}(\Omega)} \tag{10}$$

The domains under consideration.

Here we specify the meaning of the *shape of a drop*. We look for a minimum in a set of admissible domains, which are a deformation of a reference domain. We choose to work with bounded open sets Ω with Lipschitz boundary.

- We denote
$$\mathcal{C}^1(\overline{\Omega},\mathbb{R}^3) := \left\{ U_{|\overline{\Omega}} \,|\, U \in \mathcal{C}^1(\mathbb{R}^3,\mathbb{R}^3) \right\}$$
with the infinite or sup norm
$$||U||_\infty = \sup_{x\in\overline{\Omega}} |U(x)| + \sup_{x\in\overline{\Omega}} |DU(x)|$$
where DU is the differential of U.

- We introduce the set of *admissible displacements* :
$$\mathcal{U}(\overline{\Omega},\mathbb{R}^3) = \left\{ U \in \mathcal{C}^1(\overline{\Omega},\mathbb{R}^3) \,|\, ||U||_\infty < 1, U_{z|\Omega_S} \equiv 0, \text{ and } U_{|\Gamma_e} \equiv 0 \right\}$$
if $U = (U_x, U_y, U_z)$.
Finally for $U \in \mathcal{C}^1(\overline{\Omega},\mathbb{R}^3)$, $\Omega + U$ denotes the set $(Id + U)(\Omega)$.

- Let Ω^0 be a fixed reference domain of the type described in the previous paragraph. Define
$$\mathcal{D}_{ad} := \left\{ \Omega^0 + U, U \in \mathcal{U}(\overline{\Omega^0},\mathbb{R}^3) \right\}$$
the set of admissible domains we will work with.

We can formulate the problem as follows:

$$(P) \begin{cases} \text{Find } \Omega^* \in \mathcal{D}_{ad} \text{ such that} \\ J(\Omega^*) = \min\limits_{\{\Omega\in\mathcal{D}_{ad} \,|\, C(\Omega)=0\}} J(\Omega) \end{cases}$$

where $C(\Omega)$ is the volume constraint: $C(\Omega) = \text{volume}(\Omega_e \setminus \overline{\Omega}) - V$.

A necessary optimality condition. As usual, for $\Omega \in \mathcal{D}_{ad}$, and $\lambda \in \mathbb{R}$, we denote $\mathcal{L}(\Omega,\lambda) = J(\Omega) - \lambda C(\Omega)$ the Lagrangian of this constrained optimization problem. Our aim is now to find necessary optimality conditions for (Ω^*,λ^*) to be a saddle point of the given Lagrangian.

We use in the following the usual notion of shape derivatives. We refer the reader to Refs. [16,20] for details on this notion. The idea is to build a differential of a functional defined on domains. To that aim, the functional is viewed as a functional on a set of functions on which we are able to define a derivative notion.

Below, we recall the definition of shape derivative.

Definition 1.3. *A functional J defined on $\mathcal{D}_{ad}$ and with values in $\mathbb{R}$ has a directional derivative in Ω of $\mathcal{D}_{ad}$ in a direction $U \in \mathcal{U}$ if the functional $J^+ : \quad W \quad \mapsto J((I+W)(\Omega))$ defined on $\mathcal{U}(\bar{\Omega},\mathbb{R}^3)$ with values in $\mathbb{R}$ has a directional derivative at the origin 0, along the direction U (in the usual sense in $\mathcal{C}^1(\mathbb{R}^3,\mathbb{R}^3)$). The directional derivative of J in Ω in the direction U is denoted:*

$$DJ(\Omega).U := DJ^+(0).U$$

We have a necessary optimality condition:

Proposition 1.4. *If (Ω^*,λ^*) is a saddle point of $\mathcal{L}$, then if moreover J and C admit a directional derivative at Ω^* in the direction $U \in \mathcal{U}(\overline{\Omega^*},\mathbb{R}^3)$, there holds $DJ(\Omega^*).U = \lambda^* DC(\Omega^*).U$.*

The proof is rather simple and classical and can be found in this particular case for example in [28].

The next step is to prove that J is differentiable and to derive expressions of derivatives. All this has been treated in details in [28]. This is the reason why we only state the results and expressions without proofs.

Proposition 1.5. *The functionals J and C are differentiable and we have the following expressions for the derivatives:*

$$DJ_{grav}(\Omega).U = \alpha \int_\Omega U_z \, d\Omega + \alpha \int_\Omega z \, \mathrm{div}\,(U) \, d\Omega \tag{11}$$

$$DJ_{LG}(\Omega).U = \int_{\Gamma_{LG}} \mathrm{div}\,(U) \, d\Gamma - \int_{\Gamma_{LG}} < \mathbf{n}_{LG}, {}^t DU \mathbf{n}_{LG} > \, d\Gamma \tag{12}$$

$$DJ_{LS}(\Omega).U = \mu \int_{\Gamma_{LS}} \mathrm{div}\,(U) \, d\Gamma - \mu \int_{\Gamma_{LS}} < \mathbf{n}_{LS}, {}^t DU \mathbf{n}_{LS} > \, d\Gamma \tag{13}$$

$$DC(\Omega).U = \int_\Omega \mathrm{div}\,(U) \, d\Omega \tag{14}$$

$$DJ_{elec}(\Omega).U = -\frac{\delta}{2} \int_\Omega \varepsilon |\mathbf{E}^\Omega|^2 \mathrm{div}\,(U) \, d\Omega + \frac{\delta}{2} \int_\Omega \varepsilon < ({}^t DU + DU)\mathbf{E}^\Omega, \mathbf{E}^\Omega > \, d\Omega \tag{15}$$

where ${}^t DU$ is the transposition of the Jacobian of U, $\mathbf{n}_i$ is the unit outward normal vector to Γ_i for $i = LS, LG$.

The proof relies on the same arguments as in [28]. The only slight difference here is that we use a field formulation instead of a potential formulation. With the relation (7) between $\mathbf{E}^\Omega$ and $\nabla \chi_L^\Omega$, we deduce the property of differentiability directly from the arguments of proof used on $\nabla \chi_L^\Omega$.

We then can apply proposition 1.4. The necessary optimality condition will be exploited in next paragraph.

1.3. **Invariance of the contact angle**

It has already been proved in [27] (chapter 6) in every detail that the contact angle remains invariant in 3D, even for a non axisymmetric drop. In this paragraph we provide only a sketch of the proof. To simplify notations, we denote by (Ω, λ) a saddle point of the Lagrangian (i.e., we drop the *s).

The main idea is to construct a sequence of deformations U^p on Ω with compact support, that allows us to focus on the triple line as $p \to +\infty$. It is chosen such that $\frac{U^p}{||U^p||_\infty}$ is an admissible deformation, i.e. $\frac{U^p}{||U^p||_\infty} \in \mathcal{U}(\bar{\Omega}, \mathbb{R}^3)$: the underlying idea is to zoom at the triple line.

As a consequence, applying the necessary optimality condition to $\frac{U^p}{||U^p||_\infty}$, for $p \in \mathbb{N}$, we obtain

$$DJ(\Omega).U^p = \lambda DC(\Omega).U^p \tag{16}$$

Then we let p go to $+\infty$ and we scrutinize the limit of each term in Eq. (16).

Parameterization. We begin by parameterizing the domain Ω under consideration. We choose an orthonormal basis of $\mathbb{R}^3$ such that Γ_{LS} is in the plane (Oxy). We consider Γ the triple line of the drop. It is a closed curve in (Oxy) which we suppose to be of $\mathcal{C}^2$ class. We denote by l_Γ its length.

let γ be then a parameterization of Γ by the curvilinear abscissa:

$$\gamma(s) = \begin{pmatrix} \gamma_x(s) \\ \gamma_y(s) \\ 0 \end{pmatrix}, \quad \gamma'(s) = \begin{pmatrix} \gamma'_x(s) \\ \gamma'_y(s) \\ 0 \end{pmatrix}, \quad s \in [0, l_\Gamma].$$

Furthermore, we have

- $\gamma^k(0) = \gamma^k(l_\Gamma)$, $k = 0, 1, 2$, since Γ is a closed curve (*matching conditions*);
- $|\gamma'(s)|^2 = 1$ and $\gamma'(s) \cdot \gamma''(s) = 0$, $\forall s \in [0, l_\Gamma]$.

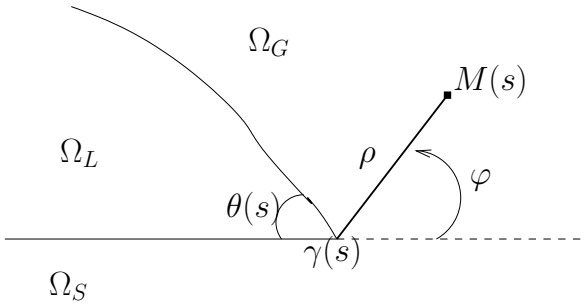

FIGURE 3. Section in the plane $\mathcal{P}_s$

For $s \in [0, l_\Gamma]$, we denote by $\mathcal{P}_s$ the plane orthogonal to $\gamma'(s)$ at $\gamma(s)$ and by $M(s)$ a point of $\mathcal{P}_s$. There exists a unique couple $(\rho, \varphi) \in]0, +\infty[\times[-\pi, \pi[$ such that:

$$\overrightarrow{OM}(s) = \gamma(s) - \rho\cos(\varphi)\gamma'^{\perp}(s) + \rho\sin(\varphi)e_z$$

where

$$\gamma'^{\perp}(s) = \begin{pmatrix} -\gamma'_y(s) \\ \gamma'_x(s) \\ 0 \end{pmatrix}$$

As a consequence

$$\overrightarrow{OM(s)} = \begin{pmatrix} \gamma_x(s) + \rho\cos(\varphi)\gamma'_y(s) \\ \gamma_y(s) - \rho\cos(\varphi)\gamma'_x(s) \\ \rho\sin(\varphi) \end{pmatrix}. \tag{17}$$

We can now give a mathematical definition to the contact angle.

Definition 1.6. *Let $s \in [0, l_\Gamma]$ be fixed. The angle $\theta(s)$ between the tangents to resp. Γ_{LG} and Γ_{LS} in the plane $\mathcal{P}_s$ is called the contact angle.*

New coordinates. We make the following hypothesis: we suppose that there exists $\rho_0 > 0$ and a small neighborhood V_{ρ_0} of the triple line such that: $\forall M \in V_{\rho_0}$, $\exists! s \in [0, l_\Gamma]$ such that $M \in \mathcal{P}_s$ and moreover its couple of coordinates (ρ, φ) in $\mathcal{P}_s$ is such that $\rho < \rho_0$.

Every $M \in V_{\rho_0}$ can then be expressed in a unique way in the coordinates system (s, ρ, φ). Let

$$\begin{array}{rccl} \chi : & \underbrace{[0, l_\Gamma]\times]0, \rho_0[\times[-\pi, \pi[}_{\mathcal{V}_{\rho_0}} & \to & V_{\rho_0} \\ & (s, \rho, \varphi) & \mapsto & \begin{pmatrix} \gamma_x(s) + \rho\cos(\varphi)\gamma'_y(s) \\ \gamma_y(s) - \rho\cos(\varphi)\gamma'_x(s) \\ \rho\sin(\varphi) \end{pmatrix} \end{array}$$

If γ is of $\mathcal{C}^2$ class, with matching conditions at $s = 0$ and $s = l_\Gamma$, then χ is differentiable and:

$$D\chi(s, \rho, \varphi) = \begin{bmatrix} \gamma'_x(s) + \rho\cos(\varphi)\gamma''_y(s) & \cos(\varphi)\gamma'_y(s) & -\rho\sin(\varphi)\gamma'_y(s) \\ \gamma'_y(s) - \rho\cos(\varphi)\gamma''_x(s) & -\cos(\varphi)\gamma'_x(s) & \rho\sin(\varphi)\gamma'_x(s) \\ 0 & \sin(\varphi) & \rho\cos(\varphi) \end{bmatrix}$$

Furthermore:

$$\det(D\chi) = -\rho(1+\rho\cos(\varphi)\det(\gamma',\gamma'')). \tag{18}$$

Let

$$D := \max_{s\in[0,l_\Gamma]} |\gamma''(s)| > 0$$

and choose $\tilde{\rho_0} = \min\{\rho_0, \frac{1}{D}\}$ so that $\det(D\chi) \neq 0$ (it is possible according to the hypotheses on γ).

We are able to represent every point M of $V_{\tilde{\rho_0}} \subset V_{\rho_0}$ uniquely in the coordinates system (s,ρ,φ). In the following we can consider the change of variables

$$\chi : \underbrace{[0,l_\Gamma]\times]0,\tilde{\rho}_0[\times[-\pi,\pi[}_{\mathcal{V}_{\tilde{\rho}_0}} \to V_{\tilde{\rho}_0}$$

and we have

$$(D\chi(s,\rho,\varphi))^{-1} = \frac{1}{\det(D\chi)} * \begin{bmatrix} -\rho\gamma_x' & -\rho\gamma_y' & 0 \\ -\rho\cos(\varphi)(\gamma_y' - \rho\cos(\varphi)\gamma_x'') & \rho\cos(\varphi)(\gamma_x' + \rho\cos(\varphi)\gamma_y'') & -\rho\sin(\varphi)(1+\rho\cos(\varphi)\det(\gamma',\gamma'')) \\ \sin(\varphi)(\gamma_y' - \rho\cos(\varphi)\gamma_x'') & -\sin(\varphi)(\gamma_x' + \rho\cos(\varphi)\gamma_y'') & -\cos(\varphi)(1+\rho\cos(\varphi)\det(\gamma',\gamma'')) \end{bmatrix} \tag{19}$$

In the rest of this part we work in this coordinates system.

General deformations. General deformations fields are given in $\mathcal{U}(\bar{\Omega},\mathbb{R}^3)$ by:

$$\begin{array}{rccc} U: & \Omega\subset\mathbb{R}^3 & \to & \mathbb{R}^3 \\ & (x,y,z) & \mapsto & (U_x(x,y,z), U_y(x,y,z), U_z(x,y,z)) \end{array}$$

Considering that this deformation is defined in the neighborhood $V_{\tilde{\rho}_0} \cap \Omega$ of the triple line, we can use the alternate coordinates system (s,ρ,φ) there.
Then we consider a particular deformation of the form $U = w\,\gamma'^{\perp}$, or:

$$U_x(s,\rho,\varphi) = U_x \circ \chi(s,\rho,\varphi) = -w(s,\rho,\varphi)\gamma_y'(s) \tag{20}$$

$$U_y(s,\rho,\varphi) = U_y \circ \chi(s,\rho,\varphi) = w(s,\rho,\varphi)\gamma_x'(s) \tag{21}$$

$$U_z(s,\rho,\varphi) = U_z \circ \chi(s,\rho,\varphi) = 0 \tag{22}$$

where w is at least of $\mathcal{C}^1$ class, with matching conditions, on the domain under consideration.

Remark 1.7. *In particular, deformations defined by (20)-(22) occur only along the x and y directions.*

Next, we build a sequence of particular deformations U^p, with compact support included in $V_{\tilde{\rho}_0}$, of the preceding form. We choose in (20)-(22) functions w^p with separated variables, and independent of φ

$$w^p : (s,\rho,\varphi) \mapsto \begin{cases} \overbrace{\exp\left(\frac{1}{\rho^2p^2-1}\right)}^{=:u^p(\rho)} v(s) & \text{if } \rho < \frac{1}{p} \\ 0 & \text{else} \end{cases} \tag{23}$$

with

– $p > \dfrac{1}{\tilde{\rho}_0}$, which ensures that the support of w^p is included in $\mathcal{V}_{\tilde{\rho}_0}$;
– v is of $\mathcal{C}^1$ class over $[0, l_\Gamma]$, with matching conditions.

In what follows, U^p is the function derived from (20)-(22) with $w = w^p$. We denote (for $p > \dfrac{1}{\tilde{\rho}_0}$)

$$\mathcal{V}_{\frac{1}{p}} := \left\{ (s, \rho, \varphi) \in \mathcal{V}_{\tilde{\rho}_0}, \text{ such that } \rho < \frac{1}{p} \right\}$$

Finally, we note that it is possible to express all differential operators (partial derivatives, divergence...) with respect to the coordinates (s, ρ, φ).

Sketch of the proof on the invariance of the contact angle. As $\frac{U^p}{\|U^p\|}$ belongs to $\mathcal{U}(\bar{\Omega}; \mathbb{R}^2)$, relation (16) is valid. We then pass to the limit in each term comprised in $DJ(\Omega).U^p$ and $DC(\Omega).U^p$, and we study carefully each contribution.

Capillary contributions. These contributions come from the terms $DJ_{LS}(\Omega).U^p$ and $DJ_{LG}(\Omega).U^p$.

- Term on Γ_{LS}

  We observe that this surface is embedded in $\{(\rho, \varphi, s) \,|\, \varphi = -\pi\}$. So, we can provide an adequate parameterization ψ of Γ_{LS}, which writes (cf. (17) with $\varphi = -\pi$):

$$\psi : (s, \rho) \mapsto \begin{pmatrix} \gamma_x(s) - \rho\gamma_y'(s) \\ \gamma_y(s) + \rho\gamma_x'(s) \\ 0 \end{pmatrix}$$

  This gives, for the elementary surface contribution $d\Gamma = \left| \dfrac{\partial \psi}{\partial s} \wedge \dfrac{\partial \psi}{\partial \rho} \right| ds d\rho$:

$$d\Gamma = (1 - \rho \det(\gamma', \gamma''))ds d\rho \tag{24}$$

  Also, $\mathbf{n}_{LS} = \begin{pmatrix} 0 \\ 0 \\ -1 \end{pmatrix}$ which yields $({}^t DU^p \mathbf{n}_{LS} \cdot \mathbf{n}_{LS}) = 0$

  After elementary calculations,

$$DJ_{LS}(\Omega).U^p = -\exp(-1) \int_0^{l_\Gamma} v(s)\, ds, \quad \forall p > \frac{1}{\tilde{\rho}_0} \tag{25}$$

  which implies

$$\lim_{p \to +\infty} DJ_{LS}(\Omega).U^p = -\exp(-1) \int_0^{l_\Gamma} v(s)\, ds. \tag{26}$$

- Term on Γ_{LG}

  We parameterize Γ_{LG}, assuming that the surface Γ_{LG} is smooth and that it can be represented by the parameterization:

$$\begin{array}{rccl} \psi : & \{(\rho, s) \,|\, 0 < s < l_\Gamma,\ \rho < \tilde{\rho}_0\} & \to & \Gamma_{LG} \\ & (s, \rho) & \mapsto & \begin{pmatrix} \gamma_x(s) + \rho\cos(\varphi(s,\rho))\gamma_y'(s) \\ \gamma_y(s) - \rho\cos(\varphi(s,\rho))\gamma_x'(s) \\ \rho\sin(\varphi(s,\rho)) \end{pmatrix} \end{array}$$

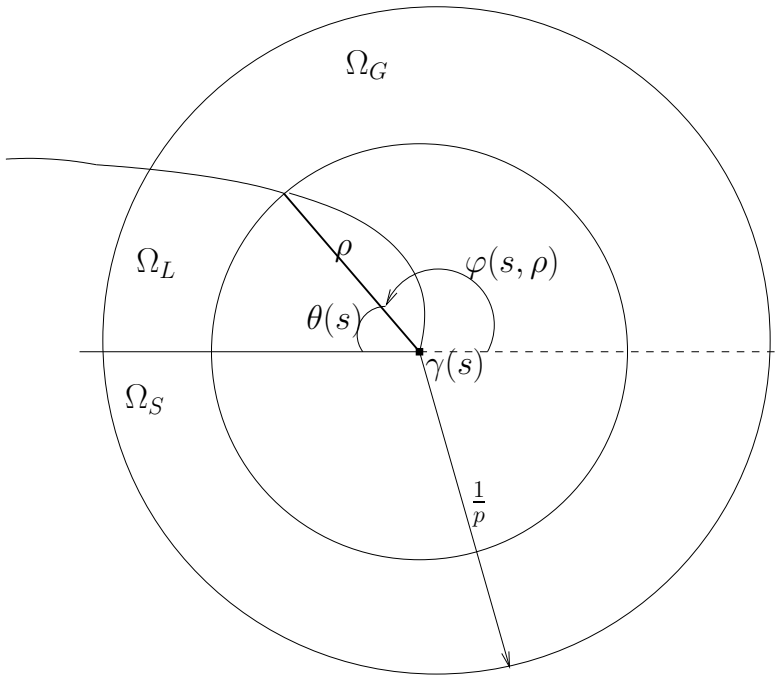

FIGURE 4. Section in the plane $\mathcal{P}_s$ of the surface Γ_{LG} (s is fixed).

with φ a function of $\mathcal{C}^2$ class, with matching conditions. We have in this case:

$$d\Gamma = \left[\left(\frac{\partial\varphi}{\partial s}\right)^2\rho^2 + \left(1+\left(\frac{\partial\varphi}{\partial\rho}\right)^2\rho^2\right)(1+\rho\cos(\varphi(s,\rho))\det(\gamma',\gamma''))\right] ds d\rho \tag{27}$$

After another sequence of elementary, but lenghty, calculations, we find:

$$\lim_{p\to+\infty} DJ_{LG}(\Omega).U^p = -\exp(-1)\int_0^{l_\Gamma}\cos(\varphi(s,0))v(s)\,ds. \tag{28}$$

Electrostatic contribution. We turn to the electrostatic term $DJ_{elec}(\Omega).U^p$. The two terms appearing in this expression are of the same type. We can thus focus on the first term, which writes:

$$\int_\Omega \varepsilon|\mathbf{E}^\Omega|^2\mathrm{div}\,(U^p)\,d\Omega.$$

It requires first the knowledge of the regularity of the electrostatic field, in terms of the Sobolev scale $H^s(\Omega)^3$, $s\geq 0$. Indeed, E^Ω is singular at the triple line, and so is $\mathrm{div}\,(U^p)$.

We are able to determine the exact behavior of the electrostatic field at the triple line. In [3], the behavior of the electrostatic potential was described, here we simply take its gradient to recover the electrostatic field:

$$\mathbf{E}^\Omega = \mathbf{E}^\Omega_{reg} + c(s)\nabla S.$$

Above, c is a smooth function of $s \in [0, l_\Gamma]$ (with matching conditions), $\mathbf{E}^\Omega_{reg}$ is regular in the sense that it belongs to $H^1(\Omega)^3$, and S is the singular part of the electrostatic potential (it belongs to $H^1(\Omega)$, but not to $H^2(\Omega)$). The expression of S is known explicitly, and it writes: $S(s, \rho, \varphi) \approx \rho^{\nu(s)}$, where ν is the unique solution in $]0, 1[$ to the equation

$$\varepsilon_S \tan(\nu(s)(\pi - \theta(s))) = -\varepsilon_G \tan(\nu(s)\pi). \tag{29}$$

Once the explicit behaviors of $\mathbf{E}^\Omega$ and $\operatorname{div}(U^p)$ are known, the study of the first term of the electrostatic contribution can be split into three parts:

$$\int_\Omega \varepsilon |\mathbf{E}^\Omega_{reg}|^2 \operatorname{div}(U^p)\, d\Omega, \quad \int_\Omega \varepsilon c(s)^2 |\nabla S|^2 \operatorname{div}(U^p)\, d\Omega \text{ and } 2\int_\Omega \varepsilon c(s) \mathbf{E}^\Omega_{reg} \cdot \nabla S \operatorname{div}(U^p)\, d\Omega.$$

The first one can be treated using the dominated convergence theorem (with the help of Sobolev imbeddings), to find a vanishing contribution when $p \to \infty$. On the other hand, the second one is treated by explicit calculations to find again a vanishing contribution. The same holds for the remaining term, by using a combination of the previous arguments. Finally, one concludes that:

$$\lim_{p\to\infty} DJ_{elec}(\Omega).U^p = 0 \tag{30}$$

Other contributions. With similar techniques, one can also show that:

$$\lim_{p\to+\infty} DC(\Omega).U^p = 0 \tag{31}$$

and

$$\lim_{p\to+\infty} DJ_{grav}(\Omega).U^p = 0. \tag{32}$$

Conclusion. Putting all the contributions (26), (28), (30), (31), (32) together, we conclude that for all v of $\mathcal{C}^1$ class over $[0, l_\Gamma]$, with matching conditions:

$$\exp(-1)\int_0^{l_\Gamma} (\mu + \cos(\theta(s))\, v(s)\, ds = 0,$$

which implies

$$\cos(\theta(s)) = -\mu, \quad \forall s \in [0, l_\Gamma]. \tag{33}$$

Therefore, the contact angle is independent of the applied potential and remains equal to Young's angle, the contact angle at $0V$, defined by $\cos(\theta_Y) = -\mu$.

2. Numerical analysis

2.1. **Finding the optimal shape**

Turning to the numerical approximation of the shape of the drop, we want to find a saddle point (Ω^*, λ^*) of the Lagrangian $\mathcal{L}(\Omega, \lambda) = J(\Omega) - \lambda C(\Omega)$ at a given potential. In order to compute it we can use a Uzawa algorithm. It requires at each step to compute the electrostatic field on a given domain Ω (the domain Ω varies from one step to the other, see figure 5). The singularity of this field near the contact line requires accurate calculations in order to compute the electrostatic part.

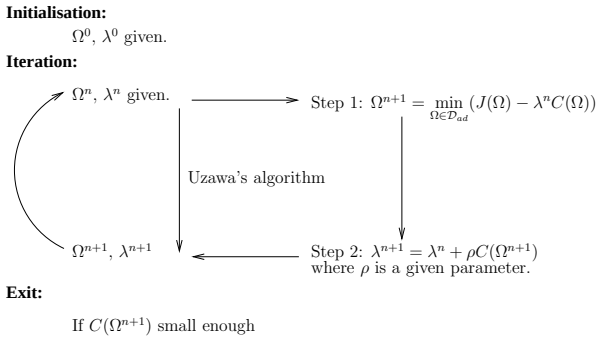

FIGURE 5. Sketch of the iteration algorithm.

Indeed during Step 1 (figure 5), one has to compute a minimum. This requires the discrete computation of $DJ(\Omega)$, $DC(\Omega)$ and of the solution to the equation $DJ(\Omega) = \lambda^n C(\Omega)$. Consequently a precise approximation of the electrostatic field is needed. In the same way as in [27], to be more accurate in the computation of the optimal domain, one could consider a coupling with a local model, which would require the evaluation of the normal trace on Γ_{LG} of the approximate electric field in the vicinity of the contact line.

As remarked before, the point of view adopted here is not the same as the one adopted in [28] and in which numerical analysis and computations have only been investigated in 3D *axisymmetric* domains. In addition, the method we investigate here relies on a (direct) numerical approximation of the field. Indeed, one computes directly an approximation of the field, whereas in [28], the idea is to obtain an accurate numerical approximation of the potential, whose gradient is calculated at a second stage.

2.2. **Weighted weak formulation**

We turn now to the design of a setting that allows us to approximate directly the electrostatic field in 3D domains. With the transmission condition (5) imposed on Γ_{GS} and with the boundary condition (3) prescribed on Γ_L and Γ_0, the electric field naturally belongs to the Sobolev space

$$\mathcal{H}_{0,\Gamma_0\cup\Gamma_L}(\mathbf{curl}\,,\Omega) := \{\mathcal{F} \in L^2(\Omega)^3 \,|\, \mathbf{curl}\,\mathcal{F} \in L^2(\Omega)^3 \text{and } \mathcal{F}\times\mathbf{n}_{|\Gamma_0\cup\Gamma_L} = 0\}.$$

Evaluation of the divergence in a weighted space. The domain Ω we are working on has a curvilinear polyhedral Lipschitz boundary. We expect the behavior of the field to be singular due to the triple line (cf. [10]). We follow Refs. [10, 12], and evaluate the divergence field in a weighted L^2 space. Let d be the distance to the triple line parameterized by γ: $d(x) = dist(x,\gamma)$. Let w_α be a smooth non-negative function of x, depending on a real parameter α. The weight w_α is chosen to behave locally as d^α in the vicinity of the triple line, and is bounded above and below by a strictly positive constant outside a fixed neighborhood of the triple line.

We then define, for $\alpha \geq 0$:

$$\begin{aligned} &L^2_\alpha(\Omega) := \{q \in L^2_{\rm loc}(\Omega) \,|\, w_\alpha\, q \in L^2(\Omega)\},\\ &||q||_{0,\alpha} := ||w_\alpha\, q||_0\,,\ (q,q')_{0,\alpha} := (w_\alpha\, q, w_\alpha\, q')_0, \end{aligned}$$

together with

$$\mathcal{X}_\alpha := \{\mathcal{F} \in \mathcal{H}_{0,\Gamma_0\cup\Gamma_L}(\mathbf{curl}\,,\Omega) \,|\, \mathrm{div}\,(\varepsilon\mathcal{F}) \in L^2_\alpha(\Omega),\ \text{ and } (\varepsilon\mathcal{F})\cdot\mathbf{n}_{|\Gamma_{ext}} = 0\}.$$

For $\alpha \in [0,1[$, one can prove that the imbedding of $\mathcal{X}_\alpha$ into $L^2(\Omega)^3$ is compact, and that the norm below is equivalent to the graph norm of $\mathcal{X}_\alpha$ [1]:

$$||\mathcal{F}||_{\mathcal{X}_\alpha} := \left(||\mathbf{curl}\,\mathcal{F}||_0^2 + ||\mathrm{div}\,(\varepsilon\mathcal{F})||_{0,\alpha}^2 + |\langle \varepsilon\mathcal{F}\cdot\mathbf{n}, 1\rangle_{\Gamma_0}|^2\right)^{1/2}.$$

We denote by $(\cdot,\cdot)_{\mathcal{X}_\alpha}$ the scalar product associated to this norm.

Remark 2.1. *The weight is introduced to recover density of the subspace of $\mathcal{X}_\alpha$ made of piecewise smooth fields in $\mathcal{X}_\alpha$ (see below for a precise statement). On the other hand, the last term $|\langle \varepsilon\mathcal{F}\cdot\mathbf{n}, 1\rangle_{\Gamma_0}|$ is added because the boundary of Ω is not connected. The existence of the normal trace (times ε) on Γ_L, Γ_{ext} and Γ_0 is guaranteed for elements of $\mathcal{X}_\alpha$, as soon as $\alpha \in [0,1[$. As a matter of fact, using the technique developed in [15] (chapter I), the normal trace of any field $\mathcal{F} \in L^2(\Omega)^3$ such that $\mathrm{div}\,\mathcal{F} \in L^2_\alpha(\Omega)$ can be defined in $H^{-\frac{1}{2}}(\partial\Omega)$ in the usual way, since one has automatically $H^1(\Omega) \subset L^2_{-\alpha}(\Omega)$ (when $\alpha \in [0,1[$).*

Let us finally introduce the spaces of piecewise regular functions, for $s > 0$,

$$PH^s(\Omega) := \{u \in L^2(\Omega)\,|\,u_j \in H^s(\Omega_j),\ j = G, S\}. \tag{34}$$

and for $s \in \mathbb{N}^*$

$$P\mathcal{C}^s(\bar\Omega) := \{u \in \mathcal{C}(\bar\Omega)\,|\,u_j \in \mathcal{C}^s(\bar\Omega_j),\ j = G, S\}. \tag{35}$$

It can be proved, as in [10][2], that there exists $\alpha_{min} \in]0,1[$ such that the space $\mathcal{X}_\alpha \cap (PH^1(\Omega))^3$ is dense in $\mathcal{X}_\alpha$, for all $\alpha \in]\alpha_{min}, 1[$. This fundamental property allows one to approximate elements of $\mathcal{X}_\alpha$ by discrete, piecewise continuous, Lagrange finite element approximations, when α belongs to $]\alpha_{min}, 1[$.

Weighted weak formulation. Now, let us focus on the original problem governing the electrostatic field. We introduce a coercive bilinear form $a(\cdot,\cdot)$, defined over $\mathcal{X}_\alpha$:

$$\begin{aligned} a(\mathcal{E},\mathcal{F}) \quad := \quad & \int_\Omega \mathbf{curl}\,\mathcal{E}\cdot\mathbf{curl}\,\mathcal{F}\,d\Omega + \sum_{i=G,S} s_d^i \int_{\Omega_i} w_\alpha \mathrm{div}\,(\varepsilon\mathcal{E}) w_\alpha \mathrm{div}\,(\varepsilon\mathcal{F})\,d\Omega \\ & + s_n \langle \varepsilon\mathcal{E}\cdot\mathbf{n}, 1\rangle_{\Gamma_0} \langle \varepsilon\mathcal{F}\cdot\mathbf{n}, 1\rangle_{\Gamma_0}. \end{aligned}$$

Above, $(s_d^i)_{i=G,S}$ and s_n are strictly positive constants, that allow one to *stabilize* the variational formulation of interest. For instance, one can choose $s_d^i = \varepsilon_i^{-2}$ for $i = G, S$ (see [10]).

Remark 2.2. *One could also use a mixed approach (with a Lagrange multiplier), as an extra means to capture an even better approximation of the divergence of the field. This topic is discussed for instance in [9].*

We then introduce a linear form $\ell(\cdot)$, defined over $\mathcal{X}_\alpha$:

$$\ell(\mathcal{F}) := -s_n \mathbb{C}V \langle \varepsilon\mathcal{F}\cdot\mathbf{n}, 1\rangle_{\Gamma_0}.$$

We now consider the weighted weak formulation below, following [7]:
Find $\mathbf{E}^\Omega \in \mathcal{X}_\alpha$ such that

$$a(\mathbf{E}^\Omega, \mathcal{F}) = \ell(\mathcal{F}),\ \forall \mathcal{F} \in \mathcal{X}_\alpha. \tag{36}$$

Proposition 2.3. *$\mathbf{E}^\Omega$ is a solution to (1)-(6) and (8) if and only if $\mathbf{E}^\Omega$ is a solution to the weak form (36).*

[1] These results can be obtained by combining arguments resp. used in [14] (mixed boundary conditions), [12] (weighted norm for the divergence), and [10] (piecewise constant ε).

[2] The problem is due to the presence of the triple line. So, one uses a localization argument, with the help of a truncation function, to reduce the problem to a neighborhood of the triple line. The result has then been obtained in [10]. In addition, we note that "explicit" computations can be carried out to characterize α_{min}, with respect to: the contrast $\varepsilon_G/\varepsilon_S$, the contact angle, and the geometry of the triple line (see §2.3).

In either case, $\mathbf{E}^\Omega$ can be written as in (7).

Proof: We easily have that if $\mathbf{E}^\Omega$ is a solution to (1)-(6) and (8), it implies in turn that $\mathbf{E}^\Omega$ is a solution to (36).

For the reciprocal assertion, let's suppose that $\mathbf{E}^\Omega$ is a solution to (36). Then $\mathbf{E}^\Omega \in \mathcal{X}_\alpha$. Next, let us take $\mathcal{F} = \mathbf{E}^\Omega + V\nabla\chi_0^\Omega$, so that $\mathcal{F} \in \mathcal{X}_\alpha$. Indeed $\nabla\chi_0^\Omega$ belongs to $\mathcal{X}_\alpha$, since it is such that:

- $(\varepsilon\nabla\chi_0^\Omega \times n)_{|\Gamma_0\cup\Gamma_L} = 0, \quad (\varepsilon\nabla\chi_0^\Omega \cdot n)_{|\Gamma_{ext}} = 0\,;$
- $\mathrm{div}\,(\varepsilon\nabla\chi_0^\Omega) = 0$ in $L^2(\Omega)\,;$
- $\mathbf{curl}\,(\nabla\chi_0^\Omega) = 0$ in $L^2(\Omega)^3$.

The weighted weak formulation applied to the test-function $\mathcal{F}$ gives:

$$\int_\Omega |\mathbf{curl}\,\mathbf{E}^\Omega|^2\,d\Omega + \sum_{i=G,S} s_d^i \int_{\Omega_i} (w_\alpha \mathrm{div}\,(\varepsilon\mathbf{E}^\Omega))^2\,d\Omega + s_n(\langle\varepsilon\mathbf{E}^\Omega\cdot\mathbf{n},1\rangle_{\Gamma_0} + \mathbb{C}V)\langle(\varepsilon\mathbf{E}^\Omega + \varepsilon V\nabla\chi_0^\Omega)\cdot\mathbf{n},1\rangle_{\Gamma_0} = 0 \quad (37)$$

But by definition of $\mathbb{C}$ and χ_0, we know that:

$$\langle\varepsilon V\nabla\chi_0^\Omega\cdot\mathbf{n},1\rangle_{\Gamma_0} = \mathbb{C}V.$$

The expression (37) then becomes:

$$\int_\Omega |\mathbf{curl}\,\mathbf{E}^\Omega|^2\,d\Omega + \sum_{i=G,S} s_d^i \int_{\Omega_i} (w_\alpha \mathrm{div}\,(\varepsilon\mathbf{E}^\Omega))^2\,d\Omega + s_n(\langle\varepsilon E^\Omega\cdot\mathbf{n},1\rangle_{\Gamma_0} + \mathbb{C}V)^2 = 0$$

which yields (as by definition $\mathrm{div}\,(\varepsilon\mathbf{E}^\Omega)$ belongs to $L^2_\alpha(\Omega)$):

$$\begin{cases} \mathbf{curl}\,(\mathbf{E}^\Omega) = 0 \text{ in } L^2(\Omega)^3\,; \\ \mathrm{div}\,(\varepsilon\mathbf{E}^\Omega) = 0 \text{ in } L^2_\alpha(\Omega)\,; \\ \langle\varepsilon\mathbf{E}^\Omega\cdot\mathbf{n},1\rangle_{\Gamma_0} = -\mathbb{C}V. \end{cases}$$

So, it follows from the first two lines that $\mathbf{E}^\Omega$ is governed by (1)-(6), and furthermore it fulfills (8) according to the last line. This ends the proof. □

As $\ell(\cdot)$ is continuous, and as the bilinear form $a(\cdot,\cdot)$ is continuous and coercive for the norm in $\mathcal{X}_\alpha$, one recovers the well-known result below.

Proposition 2.4. *There exists one and only one solution to (1)-(6) and (8).*

As we noticed earlier, this solution writes as in (7). But, in §2.2, we provided a new approach for the characterization of the electrostatic field $\mathbf{E}^\Omega$ (compared to [14]).

2.3. Approximation

Value of α_{min}. According to §1.3, we know that the contact angle at the triple line is equal to Young's angle θ_Y (see fig. 6).

From Ref. [10], we deduce that:

$$\alpha_{min} = 1 - \nu_Y$$

where ν_Y is the unique solution in $]0,1[$ to the equation (see Eq. (29)):

$$\varepsilon_S \tan(\nu_Y(\pi - \theta_Y)) = -\varepsilon_G \tan(\nu_Y\pi).$$

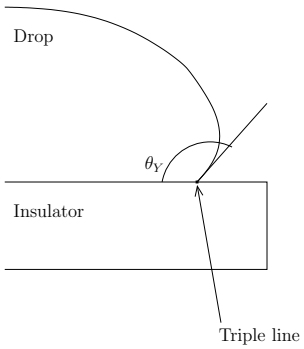

FIGURE 6. Section of the drop

In the special settings we are considering, i.e. in the case where one angle value is equal to π, one can prove the important result below (see Ref. [27] (chapter 2)).

Proposition 2.5. *For any values of the triple* $(\varepsilon_S, \varepsilon_G, \theta_Y)$*, there holds* $\nu_Y \in]1/2, 1[$.

As a consequence, we have always $\alpha_{min} \in]0, 1/2[$ and we consider from now on some $\alpha \in]\alpha_{min}, 1[$.

Discrete problem. Let $(\mathcal{T}_h)_h$ be a family of meshes of Ω, which are either made of tetrahedra, or of hexahedra. For a given mesh, the (possibly curved) volumes are called $(K_l)_l$, and the meshsize h is equal to $h = \max_{K_l \in \mathcal{T}_h} h_l$, where h_l is the diameter of the element K_l.
Let $k \geq 1$. For all h, we introduce the discretization space[3]:

$$\begin{array}{rl} \text{(tet. mesh)} & \mathcal{X}_{h,k} := \left\{ \mathcal{F}_h \in \mathcal{X}_\alpha \cap (PH^1(\Omega))^3 | (\mathcal{F}_h)_{|K_l} \in \mathbb{P}_k(K_l)^3, \, \forall K_l \in \mathcal{T}_h \right\} ; \\ \text{(hex. mesh)} & \mathcal{X}_{h,k} := \left\{ \mathcal{F}_h \in \mathcal{X}_\alpha \cap (PH^1(\Omega))^3 | (\mathcal{F}_h)_{|K_l} \in \mathbb{Q}_k(K_l)^3, \, \forall K_l \in \mathcal{T}_h \right\} . \end{array}$$

In other words, we are working with continuous Lagrange finite elements over Ω_G and Ω_S, with matching conditions at Γ_{GS}: the tangential components of the discrete fields are continuous, whereas their normal component jumps, according to the ratio $\varepsilon_G/\varepsilon_S$.
Also, we have to consider an approximate right-hand side:

$$\ell_h(\mathcal{F}_h) := -s_n \mathbb{C}^h \, V \langle \varepsilon \mathcal{F}_h \cdot \mathbf{n}, 1 \rangle_{\Gamma_0}.$$

Indeed, the one-by-one capacitance matrix on the domain Ω is not known exactly. For instance, one can use $\mathbb{P}_m$ (or $\mathbb{Q}_m$) Lagrange finite elements to approximate χ_0^Ω, and then compute

$$\mathbb{C}^h = \int_\Omega \varepsilon \nabla \chi_0^h \cdot \nabla \chi_0^h \, d\Omega.$$

[3]Numerical Analysis in the case of curved boundaries is not available, however a series of numerical experiments carried out in [13] showed that the standard numerical analysis (case of plane faces) is valid when $k \leq 5$.

The discrete problem is thus given by:
Find $\mathbf{E}_h^\Omega \in \mathcal{X}_{h,k}$ *such that*

$$a(\mathbf{E}_h^\Omega, \mathcal{F}_h) = \ell_h(\mathcal{F}_h),\ \forall \mathcal{F}_h \in \mathcal{X}_{h,k}$$

The discrete problem has a unique[4] solution in $\mathcal{X}_{h,k}$. One can also establish estimates on the rate of convergence of the method.

Proposition 2.6. *The worst case estimate between the exact and computed fields takes the form:*

$$\forall \eta > 0,\ \exists C_\eta,\ \|\mathbf{E}^\Omega - \mathbf{E}_h^\Omega\|_{\chi_\alpha} \leq C_\eta\, h^{\alpha - \alpha_{min} - \eta}. \tag{38}$$

Classically, this estimate can be improved, if one uses (locally) refined meshes, near the triple line.

Proof: The error estimate is obtained with the help of the first Strang lemma (cf. theorem 26.1 of Ref. [11]). More precisely, one has to evaluate two terms: a consistency error on the right-hand side, and an approximation error on the field.

First, one has to bound the consistency error on the right-hand side, namely

$$Err_{const}^h := \sup_{\mathcal{F}_h \in \mathcal{X}_{h,k}} \frac{|\ell(\mathcal{F}_h) - \ell_h(\mathcal{F}_h)|}{\|\mathcal{F}_h\|_{\mathcal{X}_\alpha}}.$$

Clearly, one has $Err_{const}^h \leq C_c\, s_n\, V\, |\mathbb{C} - \mathbb{C}^h|$, with C_c independent of h. So, estimating the consistency error amounts to estimating the approximation error $\|\chi_0^\Omega - \chi_0^h\|_{H^1(\Omega)}$. One finds

$$\forall \eta > 0,\ \exists C_{\eta,c},\ \|\chi_0^\Omega - \chi_0^h\|_{H^1(\Omega)} \leq C_{\eta,c}\, h^{\sigma - 1 - \eta}, \tag{39}$$

where σ is defined as the minimum singularity exponent of the Dirichlet problem with operator $\mathrm{div}\,(\varepsilon \nabla \cdot)$[5]. Interestingly, Costabel and Dauge in [12] remarked that there holds $\sigma = \nu_Y + 1 = 2 - \alpha_{min}$, so that the right-hand side of (39) is actually bounded by $C_{\eta,c}\, h^{1 - \alpha_{min} - \eta}$. One concludes that

$$\forall \eta > 0,\ \exists C_{\eta,c},\ Err_{const}^h \leq C_{\eta,c}\, h^{1 - \alpha_{min} - \eta}. \tag{40}$$

Second, one has to study the approximation error,

$$Err_{approx}^h := \inf_{\mathcal{F}_h \in \mathcal{X}_{h,k}} \|\mathbf{E}^\Omega - \mathcal{F}_h\|_{\mathcal{X}\alpha}.$$

We follow [12], taking into account that we are dealing with a "composite" domain Ω in the same sense as in [10].
The field $\mathbf{E}^\Omega$ is decomposed into a piecewise regular part and a singular part written as a gradient of a scalar, more precisely (see [10]):

$$\mathbf{E}^\Omega = \mathbf{E}_R^\Omega + \nabla \varphi^\Omega$$

with $\mathbf{E}_R^\Omega \in \mathcal{X}_\alpha \cap PH^1(\Omega)$ and $\varphi^\Omega \in H_\alpha$ where $H_\alpha := \left\{\varphi \in H^1(\Omega),\ \nabla\varphi \in \mathcal{X}_\alpha\right\}$. Moreover, this splitting is continuous. In other words:

$$\left(\|\mathbf{E}_R^\Omega\|_{PH^1(\Omega)} + \|\varphi^\Omega\|_{H^1(\Omega)} + \|\mathrm{div}\,\varepsilon\nabla\varphi\|_{0,\alpha}\right) \leq C \|\mathbf{E}^\Omega\|_{\mathcal{X}_\alpha},$$

[4] Thanks to standard convergence theory, we have $\lim_{h\to 0} \|\mathbf{E}^\Omega - \mathbf{E}_h^\Omega\|_{\chi_\alpha} = 0$.

[5] If one introduces the usual space $H_0^1(\Omega) := \{\phi \in H^1(\Omega) \,|\, \phi_{|\partial\Omega} = 0\}$, σ is such that :

$$\begin{array}{ll} \{\phi \in H_0^1(\Omega) \,|\, \mathrm{div}\,(\varepsilon\nabla\phi) \in L^2(\Omega)\} & \subset \bigcap_{s<\sigma} PH^s(\Omega), \\ \{\phi \in H_0^1(\Omega) \,|\, \mathrm{div}\,(\varepsilon\nabla\phi) \in L^2(\Omega)\} & \not\subset PH^\sigma(\Omega). \end{array}$$

with C independent of the field $\mathbf{E}^\Omega$. Furthermore, due to the geometry of the domain, there holds[6]

$$\mathbf{E}_R^\Omega \in \bigcap_{s<1+\nu_Y} (PH^s(\Omega))^3 \text{ and } \varphi^\Omega \in \bigcap_{s<1+\nu_Y} PH^s(\Omega).$$

To obtain error approximation, one needs assumptions similar to those of Ref. [12]:

(a) $\mathcal{X}_{h,k}$ has a good approximation property for the regular part of $\mathbf{E}_R^\Omega$ i.e.:
$\forall \eta > 0$, $\exists C_\eta$, $\forall \mathcal{F} \in \bigcap_{s<1+\nu_Y} (PH^s(\Omega))^3 \cap \mathcal{X}_\alpha$, $\forall h > 0$, $\exists \mathcal{F}_h \in \mathcal{X}_{h,k}$,

$$\|\mathcal{F} - \mathcal{F}_h\|_{PH^1(\Omega)} \leq C_\eta h^{\nu_Y - \eta}.$$

(b) There exists gradients in $\mathcal{X}_{h,k}$, i.e. there exists a space $\Phi_h \neq \{0\}$ such that:

$$\mathbf{grad}\ \Phi_h \subset \mathcal{X}_{h,k}$$

(c) This space has a good approximation property for the gradient part $\nabla\varphi^\Omega$.
$\forall \eta > 0$, $\exists C_\eta > 0$, $\forall h > 0$, $\exists \varphi_h \in \Phi_h$,

$$\|\varphi^\Omega - \varphi_h\|_{H^1(\Omega)} + \|\mathrm{div}\, \varepsilon \nabla \varphi^\Omega - \mathrm{div}\, \varepsilon \nabla \varphi_h\|_{0,\alpha} \leq C_\eta h^{\alpha+\nu_Y-1-\eta}$$

Then the error estimate follows (recall that $\alpha_{min} = 1 - \nu_Y$):

$$\inf_{\mathcal{F}_h \in \mathcal{X}_{h,k}} \|\mathbf{E}^\Omega - \mathcal{F}_h\|_{\mathcal{X}_\alpha} \leq C_\eta h^{\alpha - \alpha_{min} - \eta}$$

Let us consider assumption (a). If Π_h denotes the standard interpolation operator for $\mathbb{P}_k$-Lagrange finite elements, and if $\mathcal{F} \in \mathcal{X}_\alpha \cap PH^{k+1}(\Omega)$ then $\Pi_h \mathcal{F} \in \mathcal{X}_{h,k}$. Indeed due to the property of the interpolation operator, if $\mathcal{F}$ verifies transmission conditions at Γ_{GS}, so does $\Pi_h \mathcal{F}$. The same holds for boundary conditions. Then (a) is a standard consequence of well-known error estimates.

To ensure assumption (b), one should take a $\mathcal{C}^1$-conforming finite element family. More precisely, we are then looking for finite element spaces Φ_h, with corresponding polynomial space $\mathbb{P}_l$ $(1 \leq l \leq k+1)$ and global interpolant $\bar{\Pi}_h$ such that:

$$\begin{aligned} &\Phi_h \subset P\mathcal{C}^1(\bar{\Omega}) \cap H_\alpha \text{ and } \forall \varphi \in PH^{l+1}(\Omega) \cap H_\alpha,\ \bar{\Pi}_h \varphi \in H_\alpha\,; \\ &\text{a classical local approximation property holds for all } K \in \mathcal{T}_h. \end{aligned} \tag{41}$$

(The latter property is understood in the sense of almost-affine finite element, as introduced in chapter 7 of Ref. [11]).

With these hypotheses, one can prove an analogue of the estimate obtained in proposition 8.3. of Ref. [12] in terms of piecewise singular fields with transmission conditions and then obtain estimate (c). Since the method of proof used in [12] carries over to composite domains, it will not be detailed here.

It remains to give examples of such Finite Element spaces Φ_h.

- For tetrahedra-based methods: The technique is obtained by constructing macroelements. The trivariate (Hsieh-)Clough-Tocher is one example. It consists of piecewise quintic polynomial on each tetrahedron (for details see [1]). The drawback of this construction is that the interpolator operator is only defined

[6]The situation is, in a way, simpler than in [12]. Indeed, due to the absence of reentrant corners on the boundary of the domain and on the interface Γ_{GS}, the limiting regularity exponents are *automatically* identical for $\mathbf{E}_R^\Omega$ and for φ^Ω.

for $\mathcal{C}^2$ data. The degrees of freedom are indeed defined by values of the field, the normal derivative and the Hessian of the field at points of the tetrahedron. By unisolvance, this implies that transmission conditions and boundary contitions are preserved by the interpolator for a sufficiently smooth data and this yields hypothese (41). Furthermore the local approximation property is verified. This validates the use of $\mathcal{X}_{k,h}$, for $k \geq 4$.
However in a recent article by Sorokina and Worsey [29] (see also [32]) one can find a $\mathcal{C}^1$ piecewise quadratic interpolant with optimal approximation property. Due to the construction of the interpolant (which takes values of the data and its gradient at the vertices), if the data verifies transmission conditions (boundary conditions respectively) then the interpolate verifies it also. This validates the use of $\mathcal{X}_{k,h}$, for $k \geq 1$.

- For hexahedra-based methods: To our knowledge, examples of $\mathcal{C}^1$-conforming finite element families are available in 2D only. One can mention the Bogner-Fox-Schmit rectangle ($\mathbb{Q}_3$ local approximation) and the Fraeijs de Veubeke-Sander quadrilateral ($\mathbb{Q}_2$ local approximation) (see [11]). In 2D, this validates the use of $\mathcal{X}_{k,h}$, for $k \geq 2$.

Using that $\alpha_{min} = 1 - \nu_Y$, one concludes that

$$\forall \eta > 0,\ \exists C_{\eta,c},\ Err^h_{approx} \leq C_{\eta,c}\, h^{\alpha - \alpha_{min} - \eta}. \tag{42}$$

Since $\alpha < 1$, the right-hand side of (40) is negligible, compared to the right-hand side of (42), so the conclusion follows. □

Approximation of the normal trace. Along the same lines as in Remark 2.1, one notes that, by the continuity of the trace mapping on $\partial\Omega$, the error estimate (38) yields:

$$\|\varepsilon \mathbf{E}^\Omega \cdot \mathbf{n} - \varepsilon \mathbf{E}^\Omega_h \cdot \mathbf{n}\|_{H^{-\frac{1}{2}}(\partial\Omega)} \leq C_\eta\, h^{\alpha - \alpha_{min} - \eta}$$

Id est, we have at our disposal a continuous approximation of the normal trace of the field, that converges in the $H^{-\frac{1}{2}}(\partial\Omega)$-norm. Following [27], one could extend the 2D calculus to derive an ODE that describes more precisely the shape of the drop near the triple line. Indeed, this ODE uses mainly the evaluation of the normal trace (near the triple line). With the weighted approximation, an *improved* reconstruction algorithm of the shape of the drop could thus be proposed and investigated in 3D settings.

2.4. **Other choices to approximate the electrostatic field**

We review several alternate possibilities to compute the field.

H^1-conforming approximation of the electrostatic potential. This is the approach previously investigated by C. Scheid in [27] in 2D geometries: satisfactory results have been obtained. In principle, it is also usable in 3D geometries. Nonetheless, as we mentioned already, the main drawback of this method is that it does not converge numerically without the Singular Complement Method (mesh refinement is not enough). And, in a 3D non-convex geometry, we know from [17] that the SCM is not as efficient as it is in 2D. This may be caused by the fact that one approximates the potential, whereas the quantity of interest is the field, its gradient.

Different choice of applied potentials. One could choose to apply the potential V on Ω_L, and 0 on Γ_0, resulting in the same applied voltage V. Then, to characterize $\mathbf{E}^\Omega$, one has to evaluate

$$\int_{\Gamma_L} \varepsilon \mathbf{E}^\Omega \cdot \mathbf{n}\, d\Gamma.$$

However, the divergence of the field is controlled in the weighted space $L^2_\alpha(\Omega)$, with a weight w_α that goes to 0 near the triple line. As a consequence, "integrals" on Γ_L need to be handled with special care.

$\mathcal{H}(\mathbf{curl}\,,\Omega)$-*conforming approximation.* For instance, this is the situation that occurs, if one chooses edge finite elements to compute the field. In this case, one is looking for $\mathbf{E}^\Omega \in \mathcal{H}_{0,\Gamma_0\cup\Gamma_L}(\mathbf{curl}\,,\Omega)$. To enforce the conditions on the divergence (2), (4) and on the normal trace (6), (8), one must consider a *constrained setting.* To that aim, one uses scalar fields of

$$H^1_c(\Omega) := \left\{ q \in H^1(\Omega) \,|\, q_{|\Gamma_L} = 0,\ q_{|\Gamma_0} = cst \right\}, \text{with norm } |q|_1 := \|\nabla q\|_0.$$

With the help of the above mentioned conditions and integrating by parts, one finds

$$\int_\Omega \varepsilon \mathbf{E}^\Omega \cdot \nabla q \, d\Omega = -(\mathbb{C}\, V)\, q_{|\Gamma_0}, \quad \forall q \in H^1_c(\Omega).$$

Therefore, a field governed by (1)-(6) and (8) satisfies

$$\left\{ \begin{array}{ll} \displaystyle\int_\Omega \mathbf{curl}\,\mathbf{E}^\Omega \cdot \mathbf{curl}\,\mathcal{F}\, d\Omega = 0, & \forall \mathcal{F} \in \mathcal{H}_{0,\Gamma_0\cup\Gamma_L}(\mathbf{curl}\,,\Omega) \\ \displaystyle\int_\Omega \varepsilon \mathbf{E}^\Omega \cdot \nabla q \, d\Omega = -(\mathbb{C}\, V)\, q_{|\Gamma_0}, & \forall q \in H^1_c(\Omega) \end{array} \right. \tag{43}$$

Now, let us introduce the *mixed* variational formulation
Find $(\mathbf{E}^\Omega, p) \in \mathcal{H}_{0,\Gamma_0\cup\Gamma_L}(\mathbf{curl}\,,\Omega) \times H^1_c(\Omega)$ *such that*

$$\left\{ \begin{array}{ll} \displaystyle\int_\Omega \mathbf{curl}\,\mathbf{E}^\Omega \cdot \mathbf{curl}\,\mathcal{F}\, d\Omega + \int_\Omega \varepsilon \mathcal{F} \cdot \nabla p \, d\Omega = 0, & \forall \mathcal{F} \in \mathcal{H}_{0,\Gamma_0\cup\Gamma_L}(\mathbf{curl}\,,\Omega) \\ \displaystyle\int_\Omega \varepsilon \mathbf{E}^\Omega \cdot \nabla q \, d\Omega = -(\mathbb{C}\, V)\, q_{|\Gamma_0}, & \forall q \in H^1_c(\Omega) \end{array} \right. \tag{44}$$

To prove the equivalence between (1)-(6) and (8), and the mixed variational formulation (44), one can proceed for instance in two steps.

Proposition 2.7. *Let* $(\mathbf{E}^\Omega, p)$ *be a solution to (44), then* $p = 0$.

Proof: Since $p \in H^1_c(\Omega)$, we note that $\mathcal{F} = \nabla p \in \mathcal{H}_{0,\Gamma_0\cup\Gamma_L}(\mathbf{curl}\,,\Omega)$: used as a test-field in (44), it yields

$$\int_\Omega \varepsilon |\nabla p|^2 \, d\Omega = 0, \text{ i.e. } p = 0.$$

□

Proposition 2.8. $\mathbf{E}^\Omega$ *is a solution to (1)-(6) and (8) if, and only if, there exists* p *such that* $(\mathbf{E}^\Omega, p)$ *is a solution to (44).*

Proof: It is clear that if $\mathbf{E}^\Omega$ is a solution to (1)-(6) and (8), then $(\mathbf{E}^\Omega, 0)$ solves (44).
Concerning the reciprocal assertion, let $(\mathbf{E}^\Omega, p)$ be a solution to (44). Then $p = 0$ according to the previous proposition. Next, using $\mathcal{F} = \mathbf{E}^\Omega$ as a test-field in the first line of (44), one finds that $\mathbf{curl}\,\mathbf{E}^\Omega = 0$. Whereas, from the second line of (44), we infer successively that $\mathrm{div}\,(\varepsilon \mathbf{E}^\Omega) = 0$, $\mathbf{E}^\Omega \cdot \mathbf{n}_{|\Gamma_{ext}} = 0$ and $\langle \varepsilon \mathbf{E}^\Omega \cdot \mathbf{n}, 1 \rangle_{\Gamma_0} = -\mathbb{C}V$.

In other words, $\mathbf{E}^\Omega$ solves (1)-(6) and (8). □

Within the Babuska-Brezzi framework (cf. [4]), one can prove directly that the mixed variational formulation is well-posed.

Proposition 2.9. *The problem (44) is well-posed.*

Proof: One has to check the inf-sup condition and the coercivity on the kernel, which we recall below.

(i) The inf-sup condition can be written

$$\exists \beta > 0, \ \inf_{q \in H^1_c(\Omega)\setminus\{0\}} \ \sup_{\mathcal{F} \in \mathcal{H}_{0,\Gamma_0\cup\Gamma_L}(\mathbf{curl},\Omega)\setminus\{0\}} \frac{\displaystyle\int_\Omega \varepsilon \mathcal{F}\cdot\nabla q \, d\Omega}{\|\mathcal{F}\|_{\mathcal{H}(\mathbf{curl},\Omega)}|q|_1} \geq \beta. \tag{45}$$

This is achieved simply by taking, for any $q \in H^1_c(\Omega)$, the test-field $\mathcal{F} = \nabla q$. The inf-sup condition follows with $\beta = 1$.

(ii) Coerciveness of $(\mathcal{F}, \mathcal{F}') \mapsto \displaystyle\int_\Omega \mathbf{curl}\,\mathcal{F}\cdot\mathbf{curl}\,\mathcal{F}'\, d\Omega$ over the kernel

$$K := \left\{ \mathcal{F} \in \mathcal{H}_{0,\Gamma_0\cup\Gamma_L}(\mathbf{curl},\Omega), \ \int_\Omega \varepsilon\mathcal{F}\cdot\nabla q\, d\Omega = 0, \ \forall q \in H^1_c(\Omega) \right\}.$$

One checks easily that

$$K = \left\{ \mathcal{F} \in \mathcal{H}_{0,\Gamma_0\cup\Gamma_L}(\mathbf{curl},\Omega), \ \mathrm{div}\,(\varepsilon\mathcal{F}) = 0, \ \mathcal{F}\cdot\mathbf{n}_{|\Gamma_{ext}} = 0, \ \langle \varepsilon\mathcal{F}\cdot\mathbf{n}, 1\rangle_{\Gamma_0} = 0 \right\}.$$

Coercivity follows, according to [14]. □

As far as numerical approximation is concerned, let us choose for instance the first family of Nédélec's edge finite elements (cf. Refs. [18,21]) of order 1 for the field[7], and the $\mathbb{P}_1$ Lagrange finite element for the multiplier. Let $(X_{h,1}, Q_{h,1})$ denote the pair of finite element spaces on a given *tetrahedral* mesh $\mathcal{T}_h$. The discrete mixed problem writes
Find $(\underline{\mathbf{E}}^\Omega_h, p_h) \in X_{h,1}\times Q_{h,1}$ *such that*

$$\left\{ \begin{array}{ll} \displaystyle\int_\Omega \mathbf{curl}\,\underline{\mathbf{E}}^\Omega_h\cdot\mathbf{curl}\,\mathcal{F}_h\, d\Omega + \int_\Omega \varepsilon\mathcal{F}_h\cdot\nabla p_h\, d\Omega = 0, & \forall \mathcal{F}_h \in X_{h,1} \\ \displaystyle\int_\Omega \varepsilon\underline{\mathbf{E}}^\Omega_h\cdot\nabla q_h\, d\Omega = -(\mathbb{C}_h\, V)\, q_{h|\Gamma_0}, & \forall q_h \in Q_{h,1} \end{array} \right. \tag{46}$$

It is a famous property that $(X_{h,1}, Q_{h,1})_h$ forms an exact sequence, in the sense that $\nabla Q_{h,1}$ is a subset of $X_{h,1}$ for all h. Thanks to this property, one has

Proposition 2.10. *Let* $(\underline{\mathbf{E}}^\Omega_h, p_h)$ *be a solution to (46), then* $p_h = 0$.

Thanks again to the Babuska-Brezzi framework ([4]), one can also prove that the discrete mixed variational formulation is well-posed, and derive error estimates.

Proposition 2.11. *Problem (46) is well-posed. Moreover, the worst case estimate between the exact and computed fields takes the form:*

$$\forall \eta > 0, \ \exists C_\eta > 0, \ \|\mathbf{E}^\Omega - \underline{\mathbf{E}}^\Omega_h\|_{\mathcal{H}(\mathbf{curl},\Omega)} \leq C_\eta h^{1-\alpha_{min}-\eta}. \tag{47}$$

Again, this estimate can be improved, if one uses refined meshes near the triple line.

[7] For higher order approximations of the field, we refer the interested reader to the illuminating Mémoire d'Habilitation à Diriger les Recherches of F. Rapetti, see [26].

Proof: First, to obtain well-posedness, one has to check a uniform discrete inf-sup condition and a uniform coercivity on the discrete kernels, which we recall below.

The uniform discrete inf-sup condition can be written

$$\exists \beta' > 0,\ \forall h,\ \inf_{q_h \in Q_{h,1}\setminus\{0\}} \sup_{\mathcal{F}_h \in X_{h,1}\setminus\{0\}} \frac{\displaystyle\int_\Omega \varepsilon \mathcal{F}_h \cdot \nabla q_h \, d\Omega}{\|\mathcal{F}_h\|_{\mathcal{H}(\mathbf{curl},\Omega)} |q_h|_1} \geq \beta'. \tag{48}$$

This is achieved simply by taking, for any $q_h \in Q_{h,1}$, the test-field $\mathcal{F}_h = \nabla q_h$. The uniform discrete inf-sup condition follows with $\beta' = 1$.

Uniform coerciveness of $(\mathcal{F}_h, \mathcal{F}'_h) \mapsto \displaystyle\int_\Omega \mathbf{curl}\, \mathcal{F}_h \cdot \mathbf{curl}\, \mathcal{F}'_h \, d\Omega$ over the kernels

$$K_h := \left\{ \mathcal{F}_h \in X_{h,1} \mid \int_\Omega \varepsilon \mathcal{F}_h \cdot \nabla q_h \, d\Omega = 0,\ \forall q_h \in Q_{h,1} \right\}.$$

This property is much more delicate to prove: we refer to Ref. [6] (theorem 3.5) for the desired result. Well-posedness of problem (46) is achieved.

The error estimate then follows from proposition 2.16, chapter II of Ref. [4]. If one recalls that $p = 0$, it writes,

$$\|\mathbf{E}^\Omega - \underline{\mathbf{E}}_h^\Omega\|_{\mathcal{H}(\mathbf{curl},\Omega)} \leq C \inf_{\mathcal{F}_h \in X_{h,1}} \|\mathbf{E}^\Omega - \mathcal{F}_h\|_{\mathcal{H}(\mathbf{curl},\Omega)} + \underline{Err}^h_{const}. \tag{49}$$

where $C > 0$ is independent of h, and $\underline{Err}^h_{const}$ is a consistency error estimate (compare the right-hand sides of (44) and (46)).

Then, one concludes by using some approximation results for the first family of Nédélec's finite elements. One knows that $\mathbf{E}^\Omega \in \mathcal{H}(\mathbf{curl}, \Omega)$ and from §2.3, that

$$\mathbf{E}^\Omega \in PH^s(\Omega)^3 \text{ for } i = G, S, \text{ for all } s < 1 - \alpha_{min}.$$

Since $1 - \alpha_{min} > 1/2$ (see proposition 2.5 and the definition of α_{min}), one can use again theorem 3.5 of Ref. [6], to get

$$\forall \eta > 0,\ \exists C_\eta > 0,\ \inf_{\mathcal{F}_h \in X_{h,1}} \|\mathbf{E}^\Omega - \mathcal{F}_h\|_{\mathcal{H}(\mathbf{curl},\Omega)} \leq C_\eta h^{1-\alpha_{min}-\eta}$$

The consistency error being of the same type as in §2.3, $\underline{Err}^h_{const}$ is bounded as in (40), and the conclusion follows. □

3. Conclusion

We presented new ways for characterizing the electrostatic field within the electrowetting framework. We also provided some possible discretizations, based on those characterizations. This paves the way to accurate numerical experiments in realistic 3D configurations. The rate of convergence is higher for edge finite elements than for continuous Lagrange finite elements: compare $h^{1-\alpha_{min}}$ to $h^{\alpha-\alpha_{min}}$, with $\alpha < 1$. Note however, that since α can be chosen as close to one as desired, the two convergence rates can become equivalent. In the case of edge finite elements, this requires the addition of a (vanishing) Lagrange multiplier, resulting in a mixed setting. But while the error estimate is only valid in terms of the $\mathcal{H}(\mathbf{curl}, \Omega)$ norm for edge finite elements, the estimate obtained for continuous Lagrange finite elements is valid in the $\mathcal{X}_\alpha$ norm. The added feature is that it allows one to control the divergence of the field in the weighted L^2_α norm. As a by-product, one obtains an accurate approximation (in $H^{-\frac{1}{2}}(\partial\Omega)$-norm) of the normal trace (times ε) at the triple line. This is an important intermediate result to derive an improved reconstruction algorithm for the electrowetting in 3D.

References

[1] Alfeld, P.: A trivariate Clough-Tocher scheme for tetrahedral data. Comput. Aided Geom. Design, **1**, 169–181 (1984)

[2] Berge, B.: Electrocapillarité et mouillage de films isolants par l'eau. C. R. Acad. Sci. Paris Ser. II **317**, 157 (1993)

[3] Bouchereau, S.: Modelling and numerical simulation of electrowetting (in French). PhD thesis, Université Grenoble I, France (1997)

[4] Brezzi, F., Fortin, M.: Mixed and hybrid finite element methods. Springer-Verlag, Series in Computational Mathematics, **15** (1991)

[5] Buehrle, J., Herminghaus, S., Mugele, F.: Interface profile near three phase contact lines in electric fields. Phys. Rev. Lett. **91**(8) (2003)

[6] Chen, Z., Du, Q., Zou, J.: Finite element methods with matching and nonmatching meshes for Maxwell equations with discontinuous coefficients. SIAM J. Numer. Anal. **37**, 1542–1570 (2000)

[7] Ciarlet, Jr., P.: Augmented formulations for solving Maxwell equations. Comp. Meth. Appl. Mech. and Eng. **194**, 559–586 (2005)

[8] Ciarlet, Jr., P., He, J.: The Singular Complement Method for 2d problems. C. R. Acad. Sci. Paris Ser. I **336**, 353–358 (2003)

[9] Ciarlet, Jr., P., Hechme, G.: Computing electromagnetic eigenmodes with continuous Galerkin approximations. Comp. Meth. Appl. Mech. and Eng. **198**, 358–365 (2008)

[10] Ciarlet, Jr., P., Lefèvre, F., Lohrengel, S., Nicaise, S.: Weighted regularization for composite materials in electromagnetism. *Submitted.*

[11] Ciarlet, P. G. : Basic error estimates for elliptic problems, in Handbook of numerical analysis, Eds. P. G. Ciarlet and J.–L. Lions, Volume II, pp. 17–351, North Holland (1991)

[12] Costabel, M., Dauge, M.: Weighted regularization of Maxwell equations in polyhedral domains. Numer. Math. **93**, 239–277 (2002)

[13] Costabel, M., Dauge, M., Martin, D., Vial, G.: Weighted Regularization of Maxwell Equations – Computations in Curvilinear Polygons. Proceedings of Enumath'01, held in Ischia, Italy (2002).

[14] Fernandes, P., Gilardi, G.: Magnetostatic and electrostatic problems in inhomogeneous anisotropic media with irregular boundary and mixed boundary conditions. Math. Mod. Meth. Appl. Sci. **7**, 957–991 (1997)

[15] Girault, V., Raviart, P.-A.: Finite element approximation of the Navier-Stokes equations. Springer-Verlag, Berlin (1986)

[16] Henrot, A., Pierre, M.: Variation et optimisation de formes, une analyse géométrique (in French). Springer-Verlag, Mathematics and Applications, **48** (2005)

[17] Kaddouri, S.: Solution to the electrostatic potential problem in singular (prismatic or axisymmetric) domains. A multi-scale study in quasi-singular domains (in French). PhD thesis, Ecole Polytechnique, France (2007)

[18] Monk, P.: Finite Elements Methods for Maxwell's equations. Oxford Science Publications (2003)

[19] Mugele, F., Baret, J.C.: Electrowetting: From basics to applications. J. Phys.: Condens. Matter **17**, R705-R774 (2005)

[20] Murat, F., Simon, J.: Sur le contrôle optimal par un domaine géométrique (in French). Université Pierre et Marie Curie (Paris VI), Publication du Laboratoire d'Analyse Numérique (1976)

[21] Nédélec, J.-C.: Mixed finite elements in $\mathbb{R}^3$, Numer. Math. **35**, 315–341 (1980)

[22] Nicaise, S.: Polygonal interface problems, Peter Lang, Berlin, 1993

[23] Nicaise, S., Sändig, A.-M.: General interface problems I, II. Math. Meth. Appl. Sci. **17**, 395–450 (1994)

[24] Papathanasiou, A., Boudouvis, A.: A manifestation of the connection between dielectric breakdown strength and contact angle saturation in electrowetting. Appl. Phys. Lett. **86**, 164102 (2005)

[25] Quilliet, C., Berge, B.: Electrowetting: a recent outbreak. Current opinion in Colloid and Interface Science **6**, 34–39 (2001)

[26] Rapetti, F.: Higher order variational discretizations on simplices: applications to numerical electromagnetics (in French). Habilitation à Diriger les Recherches, Université de Nice, France (2008)

[27] Scheid, C.: Theoretical and numerical analysis in the vicinity of the triple point in Electrowetting (in French). PhD thesis, Université Grenoble I, France (2007)

[28] Scheid, C., Witomski, P.: A proof of the invariance of the contact angle in electrowetting. Math. Comp. Model. (2008, available online)

[29] Sorokina, T., Worsey, A.J.: A multivariate Powell-Sabin interpolant. Adv. Comput. Math. **29**, 71–89 (2008)

[30] Vallet, M., Vallade, M., Berge, B.: Limiting phenomena for the spreading of water on polymer films by electrowetting. Eur. Phys. J. B. **11**, 583 (1999)

[31] Verheijen, H., Prins, M.: Reversible electrowetting and trapping of charge: model and experiments. Langmuir **15**, 6616 (1999)

[32] Worsey, A.J., B. Piper: A trivariate Powell-Sabin interpolant. Comp. Aided Geom. Design **5**, 177–186 (1988).